Spectroscopic Studies of Electronically-Active Defects in Transition Metal Oxides for Advanced Si Devices

Gerald Lucovsky[1] and Jan Lüning[2]

[1]North Carolina State University, Department of Physics, Raleigh, NC 27695-8202, USA
[2] Stanford Synchrotron Radiation Laboratory, Menlo Park, CA, 94025, USA

Abstract. Based on spectroscopic studies, and guided by ab initio theory, the electron and hole traps in HfO_2 and other transition metal elemental oxides e.g., TiO_2, are assigned to O-atom divacancies, clustered at internal grain boundaries. *Engineering solutions* for defect reduction are identified: i) deposition of ultra-thin, < 2 nm HfO_2 and phase separated Hf silicate dielectrics, in which grain boundary formation is suppressed by effectively eliminating inter-primitive unit cell π-bonding interactions, and ii) non-crystalline Zr/Hf Si oxynitrides without nanocrystalline grain boundaries.

Keywords: transition metal oxides, x-ray absorption spectroscopy, grain-boundary defects, engineering solutions
PACS: 71.10.Ej; 73.63.Bd; 78.20.Ci; 78.70.Dm

INTRODUCTION

Densities of electrically active defects in high-k dielectrics are typically about 10-100 time higher than in Si-SiO_2 devices. A crucial issue is to determine if these defects are intrinsic or if they are derived from processing, e.g., chemical impurities. Spectroscopic studies of high-k gate dielectrics are used to identify electron and hole trapping states in HfO_2 gate stack dielectrics [1]. An asymmetry in hole and electron trapping is a significant limitation for operation and reliability of Si integrated circuits. Based on spectroscopic studies, asymmetries are explained by different charge states of O-divacancies clustered at grain boundaries in nano-crystalline (na-) films. These films are prepared at 30-300°C by remote plasma processing, RPECVD, and reactive evaporation, RE, and processed at higher temperatures (700-900°C) for device integration. Spectroscopic studies have also been performed on na-TiO_2 and -ZrO_2, and complex oxides, e.g., $La_2Ti_2O_7$, with similar results.

EXPERIMENTAL RESULTS

Soft x-ray photoelectron spectroscopy (SXPS), near edge x-ray absorption spectroscopy (NEXAS), visible and vacuum ultra-violet spectroscopic ellipsometry (vis-VUV SE), and vacuum ultra-violet photoemission spectroscopy (UPS) have been applied to na-Ti, -Zr and -Hf elemental dioxides. Figure 1(a) presents SXPS spectra for HfO_2 and TiO_2, indicating occupied defect states above the respective valence band edges. Figures 2(a) and (b) compared vis-VUV SE ε_2 spectra for TiO_2 and ZrO_2, each displaying features ~1 to 3 eV below the respective d-state band edges [2]. A comparison between the energies of d-state features extracted from the second derivative of spectra of the TiO_2 O K_1 spectrum, with energies of d-state features in the TiO_2 ε_2 spectrum yields a linear scaling relationship with a slope of 1 providing the rationale for using d-state energies extracted from O K_1 edges of HfO_2 and ZrO_2, in combination with defect state features in the XPS valence band and VUV SE ε_2 spectra, to locate the energies of defect states within the forbidden energy gaps of TiO_2, ZrO_2 and HfO_2. The correspondence between d-state features in O K_1 and ε_2 spectra is supported by hole localization in the respective final states: i) a core hole in the O 1s state, and ii) a localized hole in previously doubly occupied valence band edge O-atom 2p π state. The results of this analysis have been used to create electron energy level diagrams for HfO_2 and TiO_2 that are in excellent agreement with molecular orbital (MO) calculations applied to transition metal ion clusters [3]. Spectroscopic data for ZrO_2 yields essentially the same defect states as for HfO_2, with relatively small energy shifts. Photoconductivity and cathode-luminescence data support the intrinsic nature of these defects [2].

Experiments by our group [4], yield essentially the same asymmetric trapping as in Ref. 1. These traps are present in films prepared by RE and RPECVD, and

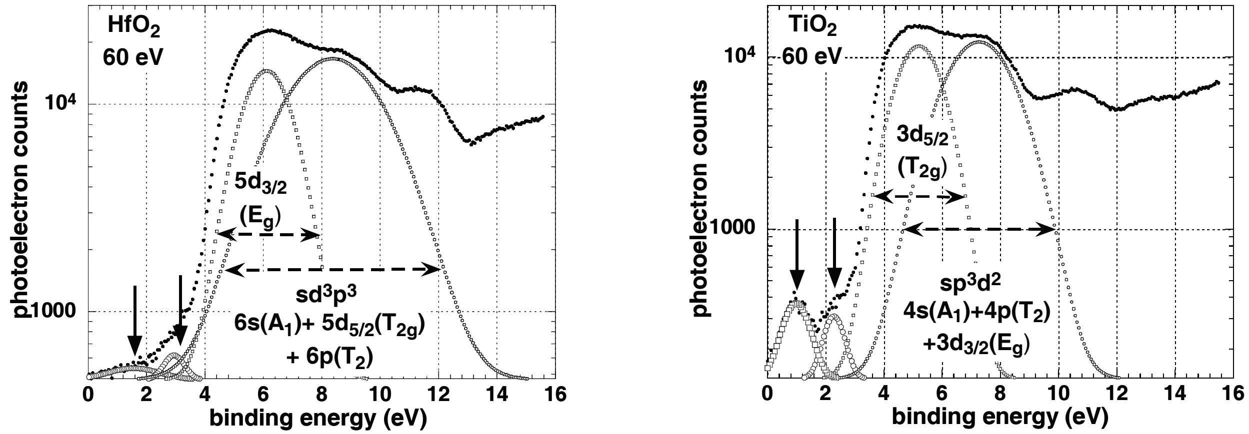

FIGURE 1. SXPS valence band spectra for na-HfO_2 and na-TiO_2, prepared by reactive evaporation.

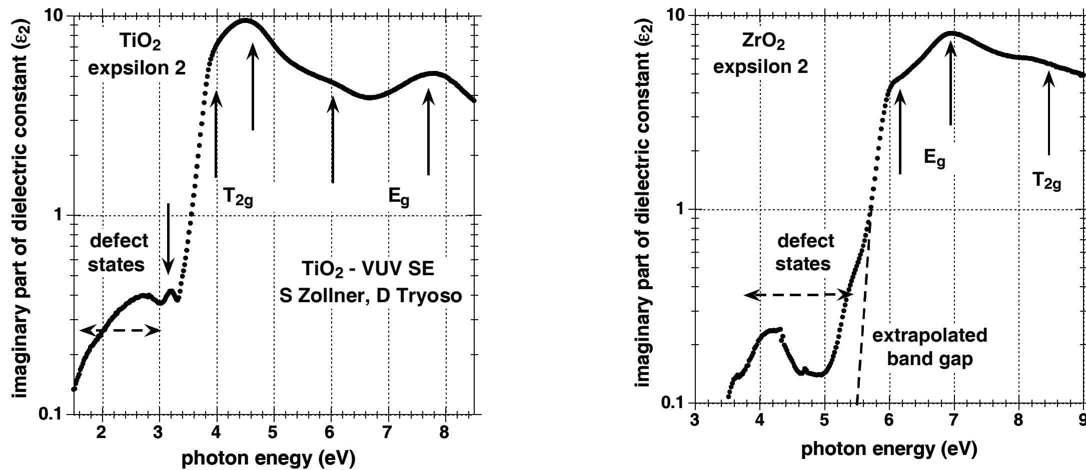

FIGURE 2. ε_2 spectra from vis-VUV-SE for (a) na-TiO_2 and (b) na-ZrO_2 films prepared by reactive evaporation.

atomic layer deposition, ALD, as well. Analysis of capacitance-voltage (C-V) and current voltage (J-V) indicate: i) relatively shallow electron traps, ~0.5 eV below the conduction band edges of HfO_2 and ZrO_2, as well as ii) deep hole traps below the valence band edge of Si; ~ 3 eV above the HfO_2 valence band.

DISCUSSION

The nature of the intrinsic defects in na-films has been identified by comparing MO calculations for octahedrally coordinated Ti^{4+} atoms in TiO_2 with Ti^{3+} in $Ti(H_2O)_6^{3+}$ clusters and Ti_2O_3, as well [3]. The defect electronic structure is *consistent with* the trap being a divacancy. Initial comparisons were based on crystal field splittings, but these have been extended to include E_g and T_{2g} state degeneracy removal by Jahn-Teller (J-T) distortions. The inherent properties of the divacancy defects are: i) electronic states of Ti^{3+} that fall within the energy gap of the Ti^{4+}-O states in TiO_2, and J-T degeneracy removal for ii) partially-occupied T_{2g} states at the valence band edge, and iii) unoccupied E_g states at the conduction band edge. The T_{2g} states of Ti^{3+} are partially occupied and act as traps for substrate hole injection, whilst E_g states are empty, and act as traps for transport via substrate injection of electrons [1], and sub-band-gap photoconductivity [2].

Similar energy level schemes apply to i) $Zr(Hf)^{3+}$ defects at grain-boundary clustered divacancies, and ii) $Zr(Hf)^{4+}$ states in bulk $Zr(Hf)O_2$ where the symmetries of the defect d-states are reversed: occupied states near the valence band are J-T term-split E_g states, and those near the conduction band, J-T term split T_g states.

Engineering solutions for elimination of these intrinsic defects have been identified. Two involve suppression of defect states in ultra-thin HfO_2 films HfO_2 films, and chemically-phase separated high HfO_2 content silicates. The third uses the deposition of non-crystalline Si_3N_4-rich Ti(Zr,Hf) Si oxynitrides: e.g.,

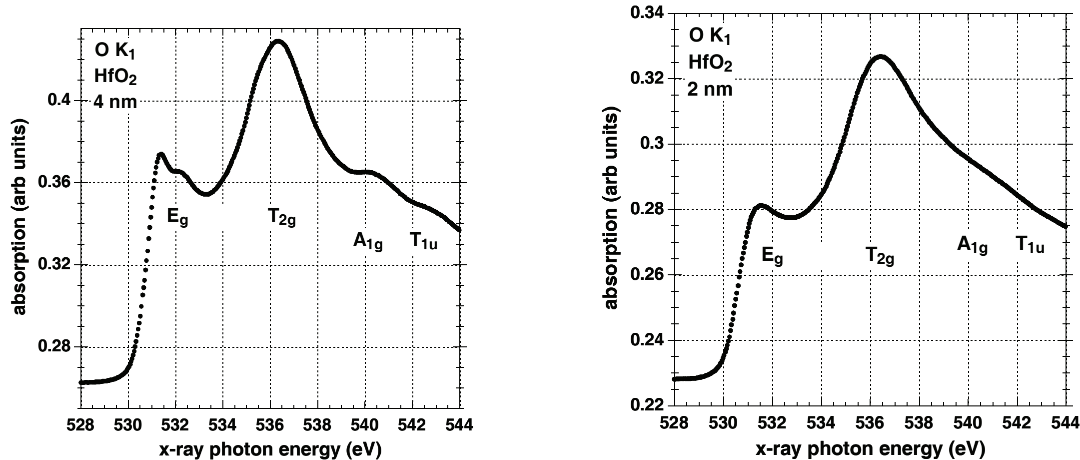

FIGURE 3. O K_1 edge spectra for na-HfO_2: (a) 4 nm thick film, and (b) 2 nm thick film.

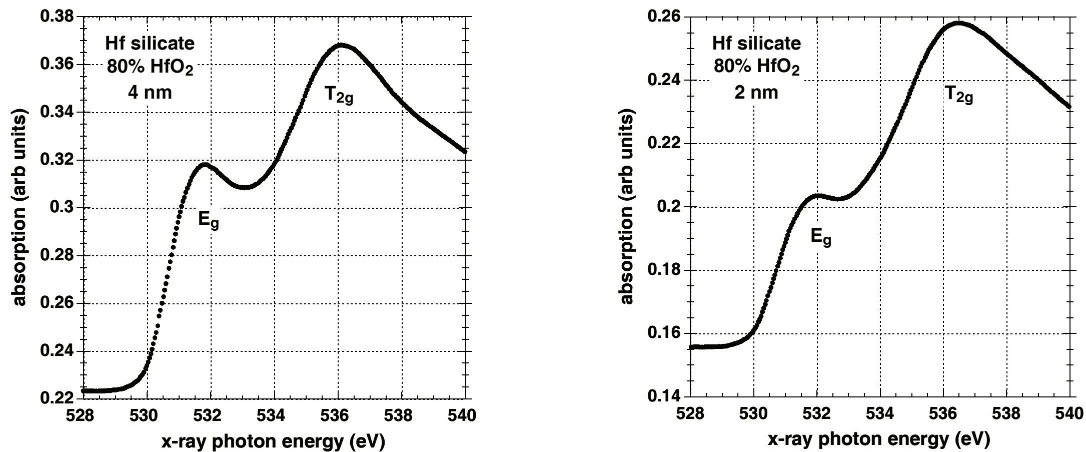

FIGURE 4. O K_1 edge spectra of phase separated Hf silicates (80% HfO_2). (a) 4 nm thick film, and (b) 2 nm thick film.

[Si_3N_4] ~33-40%, with approximately equal [SiO_2] and [Ti(Zr,Hf)O_2] concentrations of 33 to 30%.

In i) ultra-thin [<2 nm] nc-HfO_2, and ii) high HfO_2 (~80%) phase separated Hf silicates, J-T splitting of band edge E_g ($5d_{3/2}$) anti-bonding π-states is suppressed by decoupling π-bonding interactions between strings of metal and oxide atoms in neighboring *primitive unit cells* (Figs. 3(a) and (b) and 4(a) and (b)). The ~2 nm scale of order is too small for grain boundaries; however, broadening of band edge states occurs, and may effect transport properties.

Studies of O K_1 and N K_1 edges of Zr Si oxynitrides indicate 4-fold coordinated Zr with O nearest-neighbors, and Si, O and N bonding similar to Si_2ON_2. Si_3N_4 rich Zr/Hf Si oxynitrides are stable against phase separation up to 1100°C [5].

Electrical measurements show that ultra-thin HfO_2 annealed in N_2 or NH_3 at 700°C, and Zr/Hf Si oxynitrides, have low defect densities, and additionally can be scaled to EOT values of 0.7-0.8 nm, thereby extending device scaling below the 0.45 nm node [6].

REFERENCES

1. X. Zu et al.,Appl. Phys. Lett.80, 1975-1978 (2001).
2. G. Lucovsky G et. al., IEEE Trans. Dev. Mat. Reliability 5, 65-84 (2005).
3. F.A. Cotton, *Chemical Applications of Group Theory*, New York, Wiley Interscience, 1963, chap. 9.
4. G. Lucovsky G and J. Lüning, Proceedings of ESSDERC 2005 Grenoble France, 439-444 (2005).
5. B. Ju, "Properties of Zr-Si Oxynitride Dielectric Alloys" PhD. Thesis, NC State University, 2000.
6. P.D. Kirsch et al., Proceedings of ESSDERC 2005 Grenoble France, 367-370 (2005).